Biochemistry and Biophysics Reports 37 (2024) 101602

Contents lists available at ScienceDirect

Biochemistry and Biophysics Reports

journal homepage: www.elsevier.com/locate/bbrep

Statistical and network analyses reveal mechanisms for the enhancement of macrophage immunity by manganese in *Mycobacterium tuberculosis* infection

Lidong Shan [a], Zihai Wang [a], Lingshan Wu [a], Kaiqiang Qian [a], Guisen Peng [a], MeiLi Wei [a], Bikui Tang [a,b,**], Xi Jun [a,*]

[a] College of Life Science, Bengbu Medical University, China
[b] Anhui Province Key Laboratory of Immunology in Chronic Diseases, China

ARTICLE INFO

Keywords:
Manganese
RNA sequencing
Tuberculosis
Bioinformatic analysis
Regulatory net-work

ABSTRACT

Tuberculosis is a significant infectious disease that poses a serious risk to human health. Our previous research has indicated that manganese ions reduce the bacterial load of *Mycobacterium tuberculosis* in macrophages, but the exact immune defense mechanism remains unknown. Several critical proteins and pathways involved in the host's immune response during this process are still unidentified. Our research aims to identify these proteins and pathways and provide a rationale for the use of manganese ions in the adjuvant treatment of tuberculosis. We downloaded GSE211666 data from the GEO database and selected the RM (Post-infection manganese ion treatment group) and Ra (single-infection group) groups for comparison and analysis to identify differential genes. These differential genes were then enriched and analyzed using STRING, Cytoscape, and NDEx tools to identify the two most relevant pathways of the "Host Response Signature Network." After conducting an in-depth analysis of these two pathways, we found that manganese ions mainly mediate (1) the interferon -gamma (IFN-γ) and its receptor IFNGR and the downstream JAK-STAT pathway and (2) the NFκB pathway to enhance macrophage response to interferon, autophagy, polarization, and cytokine release. Using qPCR experiments, we verified the increased expression of CXCL10, MHCII, IFNγ, CSF2, and IL12, all of which are cytokines that play a key role in resistance to *Mycobacterium tuberculosis* infection, suggesting that macrophages enter a state of pro-inflammatory and activation after the addition of manganese ions, which enhances their immunosuppressive effect against *Mycobacterium tuberculosis*. We conclude that our study provides evidence of manganese ion's ability to treat tuberculosis adjuvantly.

1. Introduction

Invasion by *Mycobacterium tuberculosis* (Mtb) causes tuberculosis (TB), which can lead to pulmonary TB in the lungs and extrapulmonary TB in other parts of the body [1]. In 2021, the World Health Organization (WHO) reported that 10.6 million new TB cases occurred globally, with an incidence rate of 134 per 100,000. This included 5.6 million men, 3.3 million women, and 1.1 million children. TB is one of the leading causes of death from a single source of infection and is ranked as the 13th leading cause of death globally. In 2021, TB fatalities among HIV-negative people rose to 1.4 million, up from 1.28 million in 2020, with a mortality rate of 17/100,000, the second consecutive year of growth since 2005. According to the Global Mortality Report for 2021, the mortality rate for TB was 15%, consistent with the rate in 2020.

The strength of the host's immune system and the number, resistance, and virulence of bacteria can influence the onset, progression, and regression of tuberculosis. As *Mycobacterium tuberculosis* is an intracellular bacterium, the body's cell immunity is the primary defense against tuberculosis. However, these innate defense mechanisms are extensively modulated by Mtb to avoid host immune clearance. Among the newly discovered pathogenic mechanisms, *Mycobacterium tuberculosis* can evade host killing by altering the host's innate immune molecular regulatory mechanisms such as intrinsic cellular immunity, cellular ubiquitin system and intranuclear regulation. Multiple subtypes of immune

* Corresponding author.
** Corresponding author. College of Life Science, Bengbu Medical University, China.
E-mail address: luckymq2014@foxmail.com (X. Jun).

https://doi.org/10.1016/j.bbrep.2023.101602
Received 12 August 2023; Received in revised form 1 November 2023; Accepted 30 November 2023

cells (natural killer cells, $CD4^+$, and $CD8^+$ cells) interact with cytokines in the host's immune defense against *Mycobacterium tuberculosis*, and together they play an essential role. Macrophages, effector $CD4^+$ T lymphocytes, and the cytokine IFN-γ play an irreplaceable role, with IFN-γ primarily secreted by Th1 cells and inducing macrophage activation [2].

Organized recruitment of immune cells into *Mycobacterium tuberculosis*-infected lungs and activation of immune cells is essential for immune defense against *Mycobacterium tuberculosis*. Chemokine and cytokines help initiate and coordinate immune cells in this process. In a Mtb infection model, tumor necrosis factor α (TNFα) deficiency leads to increased susceptibility, and mice succumb to infection within 2–3 weeks while carrying a high bacterial load [3]. Although inflammatory cells accumulate at Mtb infection sites in TNFα-deficient mice, they do not merge to form granuloma tissue [4]. Genetic defects in the human IFNγ pathway are associated with an increased risk of mycosis and susceptibility to mycosis fungoides [5,6]. Patients with autosomal complete recessive IFNγR1 deficiency exhibit susceptibility to *Mycobacterium tuberculosis* infection, which manifests early in life and has a dismal prognosis [7].

Similarly, mice that do not express IFNγ due to the disruption of the target gene are susceptible to low-dose aerosol and intravenous infections and exhibit poor macrophage activation and increased granulocyte inflammation [8,9]. This suggests that IFNγ is required for the

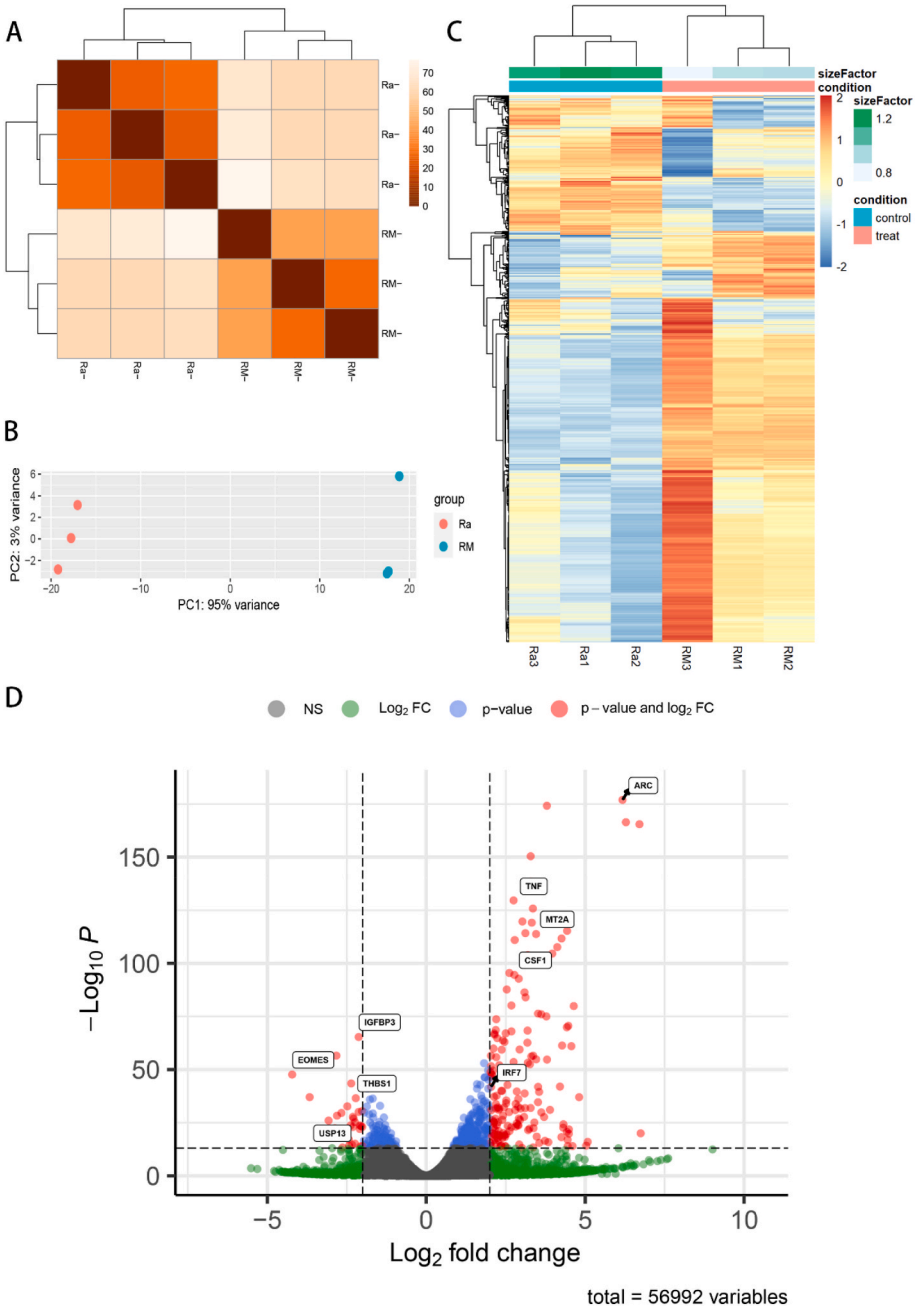

Fig. 1. Shows the differential analysis of the Mn treatment group, also known as the RM and Ra groups. Panel (A) Displays the cluster analysis of the transcriptomes of the Ra and RM groups, while Panel (B) Shows the PCA downscaling analysis of the transcriptomic data. The blue dots represent the RM group, and the red dots represent the Ra group. Panel (C) Presents the heat map of the Ra and RM groups, with blue grouping for the Ra (control) group and red grouping for the RM (treat) group. Panel (D) Shows the volcano map of differential genes in the Ra and RM group samples, with blue, green, and grey dots representing genes identified as non-differential and red dots representing genes that are significantly different.

inhibition of Mtb growth. The interleukin-10 (IL-10) family of cytokines consists of six immune mediators, namely IL-10, IL-19, IL-20, IL-22, IL-24, and IL-26. IL-10, IL-22, IL-24, and IL-26 are essential for regulating host defense against *Mycobacterium tuberculosis* infection [10].

Previous studies have found that the host cell antiviral response pathway is highly dependent on manganese (Mn) and inhibits the survival of macrophages from *Mycobacterium tuberculosis* [11]. However, the specific mechanisms remain unexplored. In this study, we used bioinformatics to analyze the transcriptomic data of macrophages treated with manganese ions after *Mycobacterium tuberculosis* infection (RM group) and compared it to those infected with *Mycobacterium tuberculosis* (Ra group). Our aim was to investigate at the molecular level how manganese ions (Mn) inhibit intracellular survival of *Mycobacterium tuberculosis*, thus reducing the bacterial load. This will provide insight into the molecular basis for reducing *Mycobacterium tuberculosis* load with Mn ion treatment and explore the potential of Mn as an adjunctive therapy for TB.

2. Results

2.1. Identification of differential genes (DEHGs)

To investigate changes in gene expression of infected macrophages after the addition of manganese ion treatment, raw reads of transcriptome data were initially processed and characterized using the R package DESeq2. This allowed us to identify DEHGs present in manganese ion treated infected macrophages compared to the control group. Cluster analysis (Fig. 1A) and principal component analysis (PCA) (Fig. 1B) revealed significant differences between the two samples. These data were visualized using MA plots, where M represents the multiple logarithmic changes on the Y-axis and A represents the average of the normalized counts on the X-axis (Fig. S1).

Eventually 1137 DEHGs were characterized with settings of $|\log2FC| > 1.5$ and p-values <0.05. This included 802 upregulated genes and 335 down-regulated genes. The 15 genes with the highest upregulated expression were *RASD1, IFNB1, AL591846.2, NGF, SCARNA9, AL158166.2, MIR320A, BEND5, RN7SKP203, ANGPTL4, BICDL2, RSPO2, CASC19, FOXJ1,* and *IFNL1*, in that order. The 15 genes with the highest downregulated expression were *AC244453.2, OTOAP1, RNU6-722P, CRISPLD1, RAD9B, AL360004.1, ANXA13, SLC26A7, CIITA, ALDH1A3, AC009974.1, GDA, EOMES, AC007406.5,* and *KCNH2* (Table 1). Complete data for upregulated and downregulated differential genes are shown in Table S1 and Table S2. Differential genes are illustrated with volcano plots (Fig. 1D).

Furthermore, a heat map of gene expression was generated which displayed different expression patterns of differential genes in H37Ra-infected cells after manganese treatment compared to mono-infected cells (Fig. 1C).

Table 1
The table of the first 15 differentially expressed host genes (DEHGs) in RM group compared to Ra group.

Up-regulate			Down-regulated		
Gene	Log2FC	Adj.pvalue	Gene	Log2FC	Adj.pvalue
RASD1	9.01	4.06E-13	AC244453.2	−5.51	0.000288
IFNB1	7.61	6.34E-09	OTOAP1	−5.32	0.000643
AL591846.2	7.57	1.63E-08	RNU6-722P	−4.79	0.005065
NGF	7.38	4.14E-08	CRISPLD1	−4.74	0.014504
SCARNA9	7.27	1.34E-07	RAD9B	−4.63	0.001719
AL158166.2	7.04	3.15E-07	AL360004.1	−4.58	0.011243
MIR320A	7.00	5.07E-08	ANXA13	−4.55	0.013306
BEND5	6.83	4.21E-06	SLC26A7	−4.53	0.011102
RN7SKP203	6.74	1.06E-20	CIITA	−4.51	6.99E-13
ANGPTL4	6.71	3.32E-166	ALDH1A3	−4.46	0.014543
BICDL2	6.59	4.70E-06	AC009974.1	−4.45	0.013509
RSPO2	6.53	1.99E-05	GDA	−4.44	0.014137
CASC19	6.52	2.49E-05	EOMES	−4.22	2.27E-48
FOXJ1	6.44	1.85E-05	AC007406.5	−4.22	0.006347
IFNL1	6.43	1.37E-06	KCNH2	−4.14	0.00929

2.2. Functional enrichment of differential genes (DEHGs) using different databases

This study investigated the biological processes and changes in fundamental biological pathways in macrophages infected with H37Ra after Mn treatment. GO analysis of biological processes showed that differential genes were mainly associated with positive regulation of cytokine production, response to oxygen levels, hypoxia, and the hexose metabolic process (Fig. 2A). GO analysis of molecular function indicated that differential genes were primarily associated with signaling receptor activator activity, receptor-ligand activity, cytokine receptor activity, cytokine receptor binding, cytokine activity, growth factor receptor binding, and cytokine binding. These associations were not enriched in the cellular component of GO. KEGG pathway analysis revealed significant enrichment of differential genes in the cytokine-cytokine receptor interaction, viral protein interaction with cytokine and cytokine receptor, JAK-STAT signaling pathway, rheumatoid arthritis, and HIF-1 signaling pathway (Fig. 2B).

BIOCARTA pathway analysis revealed significant enrichment of differential genes in cytokines and inflammatory response, selective expression of chemokine receptors during T cell polarization, erythrocyte differentiation pathway, hypoxia, and p53 in the cardiovascular system. DISEASE annotation analysis showed significant enrichment of differential genes in type 2 diabetes, chronic renal failure, Alzheimer's disease, and prostate cancer. In Table 3 we present a complete list of the results of the annotation analysis of GO, KEGG, BIOCARTA, and DISEASE for the differential genes.

2.3. Building and analysis of SiHgrn network

A PPI (protein interaction) network with 831 nodes and 919 connecting lines was obtained by searching 1137 differential genes in the STRING database and setting the PPI to 0.7. Details of the PPI network are given in Table S4. The data from the PPI network was then imported into Cytoscape software for visualization, each node in the obtained network represents a protein, and the edges represent protein interactions. Moreover, the degree of betweenness, centrality, clustering coefficient, and centrality of closeness of the SiHgrn network were calculated with the NetworkAnalyzer plugin. Then the corresponding node sizes were set according to the DEHGs'. The full results for the DEHG network topology are shown in Table S5.

2.4. Identification and analysis of key subnetworks in SiHgrn

The SiHgrn network was imported into Cytoscape, and the network was analyzed in more detail using its plugin MCODE, yielding five subnetworks (Fig. 2D; Table 2). One of the clusters with the highest MCODE score was 10.957 and contained 24 genes. Cluster 1 was subsequently selected for additional analysis. Genes for highly connected hubs can affect the biological and topological functions of networks. The TNF nodes were found to have the highest connectivity in the SiHgrn network [degree = 39]. The top 20 hub nodes in terms of connectivity were HIF1A, PLCG1, CXCR4, KAT2B, ERBB2, EGR1, CCL2, HIST2H2AC, IRF4, LIF, IRF7, THBS1, IFIT1, HIST1H4F, MET, CSF3, CSF2, IFIT2 (Table S6). Most of these apical hub genes in this study were found to be highly interrelated and belonged to cluster 1 of the MCODE (Fig. 2D; Table 2).

Functional enrichment analysis of Gene Ontology Biological Processes for group 1 genes revealed that they are mainly associated with response to virus, response to type 1 interferon, and cellular response to type 1 interferon pathways (Fig. 3A). GO analysis indicated that genes in group 1 were mainly associated with signaling receptor activator activity, receptor-ligand activity, and cytokine receptor binding (Fig. 3A).

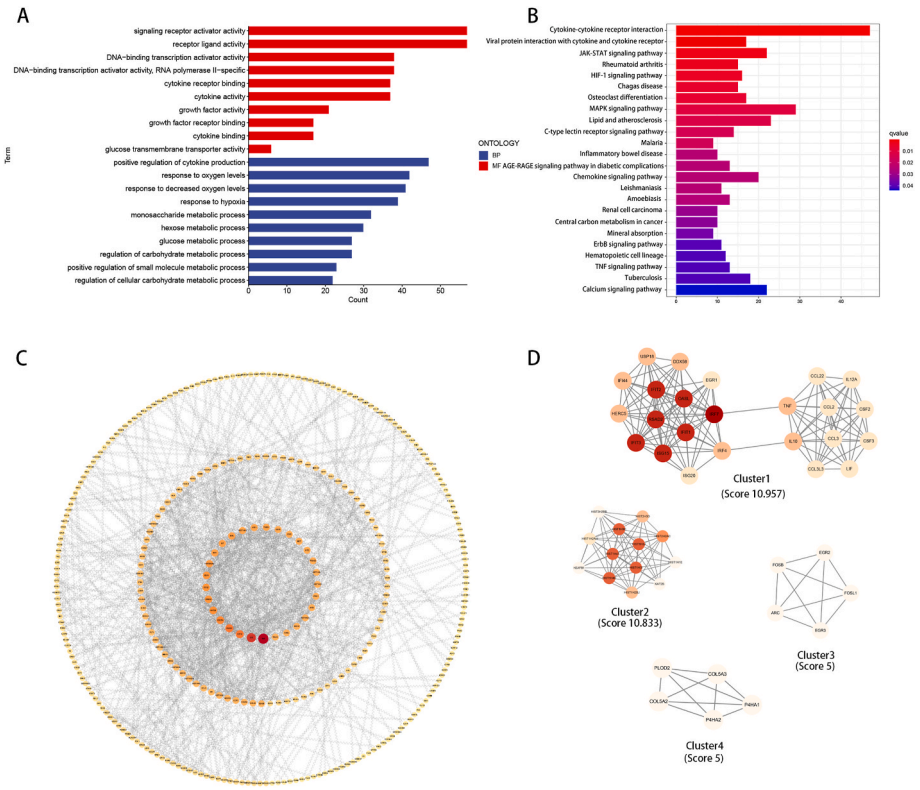

Fig. 2. Shows the functional enrichment of differential genes in the Ra and RM groups and their biological networks. Panel (A) Represents functional enrichment of differential genes with GO, while panel (B) Represents functional enrichment with KEGG. Panel (C) Shows the analysis network with Cytoscape tool and mapping of network structure. The size and color shade of each point represents the numerical size of the Degree for that gene. Panel (D) Displays the analysis of STRING network with Cytoscape plugin MCODE to obtain the top 4 clusters.

Table 2
Table of MCODE clusters found after importing SiHgrn and the proteins they contain.

Cluster	Score (Density*# Nodes)	# Nodes	# Edges	Node IDs
1	10.957	24	126	CSF3, IFI44, IL10, CSF2, DDX58, IRF7, CCL22, IFIT3, HERC5, LIF, CCL2, IFIT1, ISG20, CCL3, EGR1, ISG15, OASL, IL12A, IFIT2, IRF4, RSAD2, TNF, CCL3L3, USP18
2	10.833	13	65	HIST1H3J, HIST2H3D, HIST1H1E, HIST1H3I, HIST3H2BB, KAT2B, HIST1H4F, H2AFB1, HIST1H2BJ,HIST1H4C, HIST1H2AH, HIST2H2AC, HIST1H3C
3	5	5	10	FOSB, FOSL1, ARC, EGR2, EGR3
4	5	5	10	COL5A2, PLOD2, P4HA1, COL5A3, P4HA2
5	4.5	5	9	MT1F, MT1X, MT2A, MT1G, MT1E

The Cellular Component of the Cluster 1 gene GO was not enriched. KEGG pathway analysis of cluster 1 showed significant enrichment in Cytokine-cytokine receptor interaction, Viral protein interaction with cytokine and cytokine receptor, Chagas disease, Malaria, RIG-I-like receptor signaling pathway, and Coronavirus disease-COVID-19 (Fig. 3B). BIOCARTA analysis indicated that cluster 1 was markedly enriched in Erythrocyte Differentiation Pathway, Cytokines and Inflammatory Response, and Dendritic cells in regulating TH1 and TH2. Disease annotation analysis revealed that cluster 1 genes were markedly enriched in asthma, multiple sclerosis, type 2 diabetes, and respiratory syncytial virus bronchitis. Detailed data from GO, KEGG, BIOCARTA, and DISEASE are preserved in Table S7.

2.5. Identification of upstream regulators for cluster 1

To activate the immune response to bacterial infection, cells can rapidly regulate gene expression through transcription factors. Identifying transcription factors could improve our understanding of immune regulation and explain the role of manganese ions in controlling the intracellular survival of H37Ra and enhancing host immunity. Therefore, we analyzed the cluster 1 gene using Cytoscape's iRegulone plugin to identify its potential upstream TF regulators. The results showed that the majority of cluster 1 genes upregulated in response (log2FC > 1.5) in manganese ion-treated H37Ra-infected macrophages were controlled by the transcription factors *IRF1, STAT1, IRF3, STAT2,* and *NFkB1* (Fig. 3C). We refer to the ensemble of cluster 1 genes and their upstream transcription factors as the "Host Response Signature Network."

2.6. Uploading the "host response signature network" to NDEx for biological pathway enrichment analysis

To obtain a list of relevant pathways enriched by NDEx based on similarity scores, the genes of the "Host Response Signature Network" were analyzed using NDEx. In order of similarity, the top eight pathways had more than five genes in common with our genes (Table 3). A significant correlation was observed with the pathway "Immune response to tuberculosis" [similarity score = 0.20; overlap genes = 5; p = 2.22e-7] (Table 3 and Fig. 4), which had the highest similarity score. On the other hand, the pathway with the highest overlap genes with the "host response marker network" was the "SARS-CoV-2 innate immunity evasion and cell-specific immune response" [similarity score = 0.16; overlap genes = 12; p = 5.10e-16] (Fig. 5 and Table 3).

Table 3
Using NDEx v2.4.5 to enrich Biological Pathways in the "Host Response Characterization Network".

Pathway Name	Pathway Properties	Number of overlap gene	p-value <	Similarity score
WP4197-Immune response to tuberculosis (*Homo sapiens*) https://classic.wikipathways.org/index.php/Pathway:WP4197 Source: wikipathways	Nodes:48; Egde:30	5 genes	2.22e-7	0.20
WP4891-COVID-19 adverse outcome pathway (*Homo sapiens*) https://classic.wikipathways.org/index.php/Pathway:WP4891 Source: wikipathways	Nodes15; Egde:6	5 genes	2.57e-8	0.20
WP619-Type II interferon signaling (IFNG) (*Homo sapiens*) https://classic.wikipathways.org/index.php/Pathway:WP619 Source: wikipathways	Nodes79; Egde:83	6 genes	3.28e-8	0.18
WP5039-SARS-CoV-2 innate immunity evasion and cell-specific immune response (*Homo sapiens*) https://classic.wikipathways.org/index.php/Pathway:WP5039 Source: wikipathways	Nodes80; Egde:80	12 genes	5.10e-16	0.16
WP5095- Overview of proinflammatory and profibrotic mediators (*Homo sapiens*) https://classic.wikipathways.org/index.php/Pathway:WP5095 Source: wikipathways	Nodes152; Egde:7	11 genes	4.02e-12	0.14

The genes of the "host response signaling network" were also enriched for other immune-related pathways, including the "COVID-19 adverse outcome pathway" [similarity score = 0.20; overlap genes = 5; p = 2.57e-8] (Table 3); "Type II interferon signaling (IFNG)" [similarity score = 0.18; overlap genes = 6; p = 3.28e-8] (Table 3); "SARS-CoV-2 innate immunity evasion and cell-specific immune response" [similarity score = 0.16; overlap genes = 12; p = 5.10e-8] (Table 3); "SARS-CoV CYTOKINE STORM" [similarity score = 0.16; overlap genes = 8; p = 5.19e-8] (Table 3 and Figure SA); "Overview of pro-inflammatory and profibrotic mediators" [similarity score = 0.14; overlap genes = 11; p = 4.02e-8]. We also discovered that many of the enriched pathways were related to immunity to SARS-CoV infection, which suggests that the intracellular responses elicited by coronavirus and Mycobacterium TB infections are very similar. Co-infection triggers a more intense immune response, and co-infected individuals may suffer more severe organismal damage and sequelae than monoinfected individuals. In this regard, it is necessary to investigate whether manganese ion inhibits coronavirus.

2.7. Validation of bioassay results by qRT-PCR

We validated the expression of five mRNAs, IFNγ, IL12, CSF2, CXCL10 and MHCII, in the Ra and RM groups, respectively. As expected, our findings were consistent with our analytical results, with higher and statistically significant expression levels of CXCL10, MHCII, IFNγ, CSF2, and IL12 in the RM group compared to the Ra group (see Fig. 6). Therefore, we have presented substantial evidence to support our findings.

3. Discussion

In this study, we investigated potential regulatory mechanisms by which manganese enhances macrophage innate immunity to reduce the intracellular survival of *Mycobacterium tuberculosis*. We used RNA-Seq data and statistical analysis of computational methods to identify differential genes in H37Ra-infected macrophages treated with manganese ions. We identified 1137 differential genes, which were significantly enriched in cytokine production upregulation, cytokine interactions, cytokine receptors, and interaction of viral proteins with cytokines, as well as the JAK-STAT signaling pathway (Fig. 2A). These results suggest that cytokines play a significant role in this experiment. Cytokines are small, soluble proteins produced by cells that affect other cells' physiological activity, mainly in a paracrine manner. The family of tumor necrosis factors, interleukins, and chemokines are the main cytokines. Most of the mechanisms that maintain homeostasis in the body depend on cytokine production and response, which are produced by every nucleated cell [12]. Cytokines can bind to receptors on the surface of the cell membrane and then activate signaling pathways, such as the JAK-STAT signaling pathway and the P53 signaling pathway, and play a crucial role in cell proliferation, differentiation, and immune regulation [13]. We also enriched the type 1 interferon pathway, which is required for host immune defense responses in the pathogenesis of tuberculosis, with interferon increasing the cellular activity of natural immune cells, including macrophages, cytotoxic lymphocytes (CTL) cells, and natural killer (NK) cells.

To elucidate the interactions between individual genes and pathways, we uploaded the differential genes to STRING, integrated them with human PPI to generate the SiHgrn network (Fig. 2C), and analyzed them by CytoScape's plugin MCODE to obtain Cluster 1 with the highest clustering score (Fig. 2D). Subsequently, we performed an enrichment analysis of Cluster 1 genes showing that they were mainly enriched in pathways such as cytokine-cytokine receptor interactions, response to viruses, and response to type 1 interferon (Fig. 3A and B). This suggests that the genes in Cluster1 play a significant role in the induction of inflammation. Moreover, most of the genes in Cluster1 belong to cytokines and chemokines such as TNFα, IL10, IL12A, CSF2, and some genes of the CCL family, which were able to trigger a robust inflammatory response (Table 2). Among them, TNF-α was one of the first cytokines identified concerning tuberculosis and is essential for infection control [14]. TNF-α indirectly maintains the structure of the granuloma by limiting *Mycobacterium tuberculosis* in mouse and zebrafish infection assays [15,16]. Like TNFα, CSF2 has potential antimicrobial effects, and Csf2 −/− infected mice also had a significantly higher lung bacterial load compared to wild-type mice [17]. IL10 acts as an anti-inflammatory cytokine that down-regulates the innate and acquired immune response. Although it can suppress harmful inflammation in the context of an excessive inflammatory response, it can also harm the host by preventing effective responses [18,19].

We then used Cytoscape's iRegulone tool to analyze the Cluster1 genes and obtain the upstream regulators of these genes: *STAT1, STAT2, IRF1, IRF3,* and *NFKB1* (Fig. 4). We referred to the network of Cluster1 genes and their five upstream regulators as the "host response signature network." We then used the web analysis tool NDEx to analyze this network to identify changes in key pathways of infection and immunity following treatment of H37Ra-infected macrophages with manganese ions (Table 3).

This study performed an enrichment analysis of the "host response signature network." The "Immune response to tuberculosis" pathway showed the highest correlation [similarity score = 0.20]. This pathway is closely related to STAT1, STAT2, and the subsequent IRF1, IFIT1, and IFIT3 genes in the JAK-STAT pathway. During early TB infection, STAT1 has been shown to be activated by phosphorylation to promote transcriptional activation by downstream apoptotic factors. Additionally, STAT1 plays a vital role in promoting macrophage polarization into M1-type macrophages, which are more effective in removing Mtb through

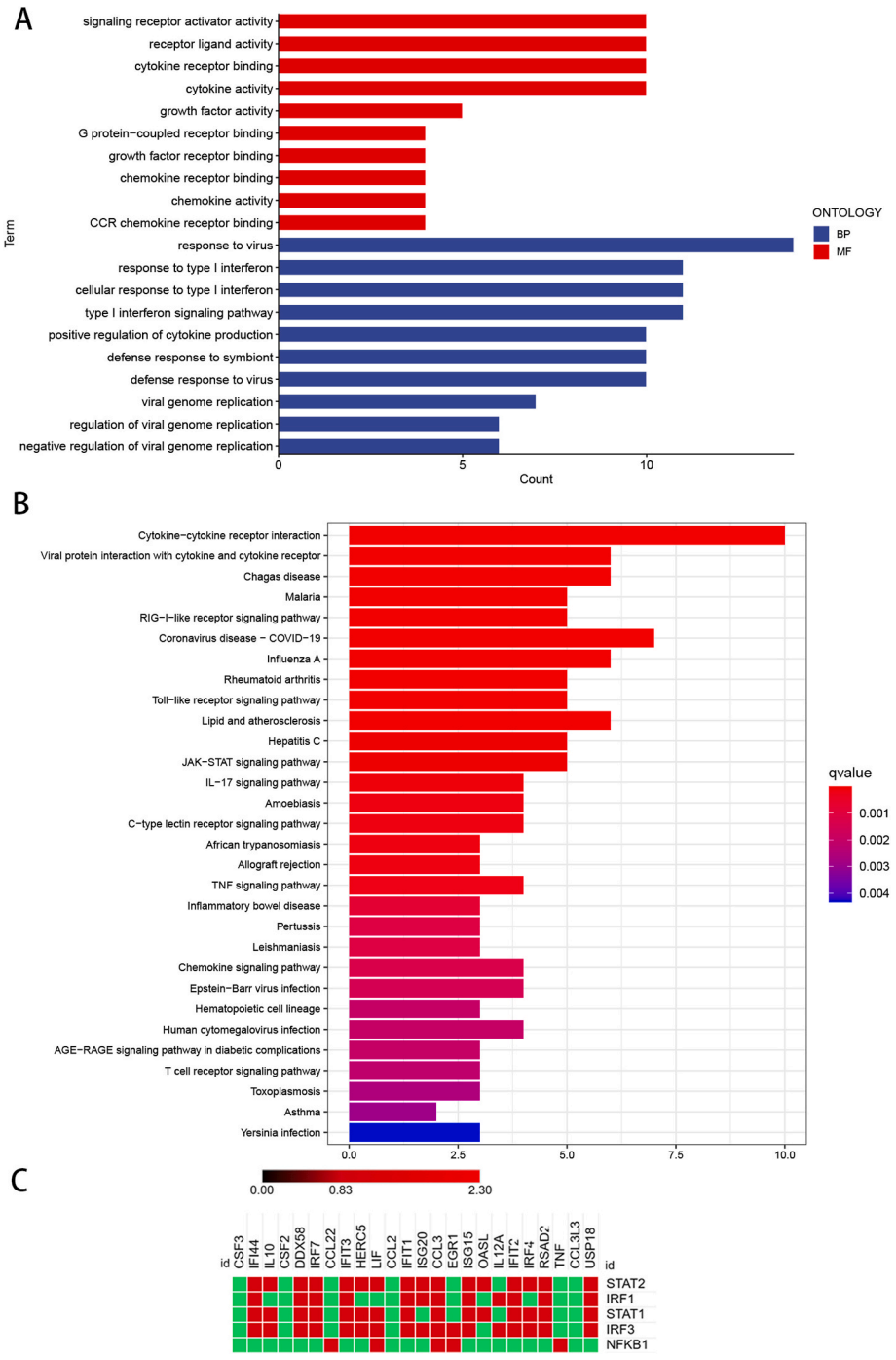

Fig. 3. Functional enrichment analysis of Cluster1 gene (A) Functional enrichment of Cluster1 gene with GO (B) Functional enrichment of Cluster1 gene with KEGG (C) Identification of upstream regulators for all genes in cluster 1. The columns represent Cluster 1 genes, and the row names represent TFs identified using iRegulone, where the TFs bound to the mRNA are indicated in red and those not bound are indicated in green.

immune function compared to M2-polarized macrophages [20,21]. IFNγ and IFNα, and IFNβ can activate the downstream JAK-SATA pathway to cause STAT phosphorylation, which is important for protective immunity against *Mycobacterium tuberculosis* [22].

IRF1, a member of the interferon regulatory factor (IRF), plays a vital role in the development of myeloid cells and in enhancing the response of myeloid cells to IFN-γ. The binding of IFN-γ to its receptor leads to the binding of IFN-γ receptors [23]. It activates the expression of IRF1 and IRF8, nuclear translocation, and transcriptional activity, which are essential for activating the full microbicidal potential of macrophages [24,25]. Moreover, IFNγ-mediated autophagy can induce inhibition of the survival of the macrophage line Mtb. Human IRF1 has been shown to be essential for IFNγ-dependent macrophage immunity against *Mycobacterium avium* and that macrophages with mutations in the IRF1 gene are more susceptible to infection by intracellular pathogens [26,27].

Macrophages play an essential role in innate and adaptive immune responses and, therefore, can help the body control bacterial infections. However, macrophages are the main ecological niche for the growth and multiplication of *Mycobacterium tuberculosis*, which is caused by the ability of *Mycobacterium tuberculosis* to alter and inhibit intracellular killing and antigen presentation mechanisms of macrophages [28–30]. In the present study, the "host response signature network" was

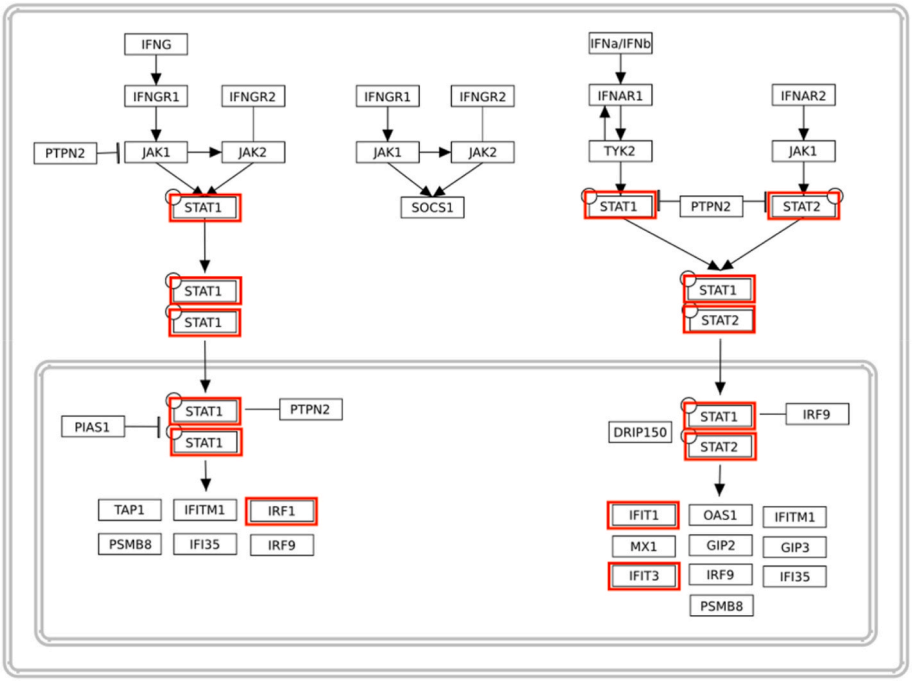

Fig. 4. The most similar pathway obtained after enrichment of the biological pathways of the "Host Response Characterization Network" was "Immune Response to Tuberculosis".

significantly correlated with "SARS-CoV-2 innate immunity evasion and cell-specific immune response" with a p-value of 5.10e-16. *Mycobacterium tuberculosis* infection triggers two signaling cascades in the innate immune system: one through NF-κB1-mediated pathways that stimulate the production of pro-inflammatory cytokines (CSF2, IL-10, and TNF); the other through interferon regulatory factors (IRF 3 and IRF 7) that stimulate the production of type I and type III IFNs [28,31,32]. We then mined the data and literature to suggest that manganese ions enhance the killing of *Mycobacterium tuberculosis* by enhancing the secretion of interferons and cytokines by macrophages.

In the cytoplasm, NF-κB proteins are typically bound by members of the IκB family and related proteins, inhibiting their function [33,34]. NF-κB is activated by two main signaling pathways, both typical and atypical, both of which play critical regulatory roles in immunity and inflammation. The typical NF-κB pathway responds to many stimuli, including ligands for various cytokine receptors, pattern recognition receptors (prr), members of the TNF receptor (TNFR) superfamily, as well as t-cell receptors (TCR), and b-cell receptors [35,36]. NF-κB not only regulates the inflammatory response, but also induces increased expression of various pro-inflammatory genes in natural immune cells and regulates the activation, differentiation and effector functions of inflammatory T cells [37]. Recent studies have also shown that NF-κB can play a regulatory role in activating inflammatory micro problems.

NF-κB can have a pro-inflammatory effect on the host against tuberculosis by promoting macrophage activation and the release of various cytokines (IL-1, IL6, IL12, and TNFα) in the macrophage infection by *Mycobacterium tuberculosis* [38]. Previous studies have shown that treatment with manganese ions after *Mycobacterium tuberculosis* infection increases the susceptibility of cGAS to cytoplasmic *Mycobacterium tuberculosis* DNA, thereby increasing the activation of cGAS-STING-TBK–NF–κB and causing an immune response and cytokine release in cells [11]. Our study found that manganese ions activated NF-κB, translocated into the nucleus, and increased the expression of TNF-α, IL-10, and CSF2 downstream of infected macrophage cells. It plays an irreplaceable role in immunity against *Mycobacterium tuberculosis*.

Based on the accumulation of experimental data and literature discovery, our findings suggest that treating *Mycobacterium tuberculosis*-infected macrophages with specific concentrations of manganese ions can promote the killing effect of macrophages against *Mycobacterium tuberculosis* by promoting (1) the interferon expression signaling pathway and (2) the NF-κB-mediated cytokine expression pathway. Macrophages in the presence of manganese ions may enhance the antimicrobial capacity of macrophages through two pathways, JAK-STAT1 and NF-κB, such as promoting macrophage polarization toward M1 type, promoting downstream inflammatory factor release, and inhibiting M2 type polarization. These results provide some new understanding for our future work on the inhibition of *Mycobacterium tuberculosis* proliferation by manganese ions, as well as theoretical support for manganese ions as a new immunoadjuvant or even a synthetic drug.

4. Materials and methods

4.1. RNA data acquisition and data processing

In this study, we used transcriptomic data from manganese ion-treated human macrophages infected with *Mycobacterium tuberculosis* as the treatment group, and *Mycobacterium tuberculosis*-infected human macrophages as the control group. We downloaded the transcriptome data from the GEO database (www.ncbi.nlm.nih.gov/geo/) by searching for GSE211666 for subsequent analysis. To identify differential genes in the treatment and control groups, we used the DESeq2 (1.32.0) package in version R4.1.1. Two files were required to run DESeq2: (i) Table of raw reads for two sets of samples, with rows representing one gene and columns representing one sample; (ii) A phenodata file was used to describe the experimental grouping with which each sample was then located. DESeq2 adjusted the size of the library and the differences in the composition of the library by performing internal normalization. DESeq2 was first used to analyze each sample to determine the scale factor. The raw reading of the sample was then divided by the scale factor to give a normalized value. DESeq2 processes each gene using a negative binomial distribution to simulate the counts and fit the normalized count data. A Wald test was used to determine whether there

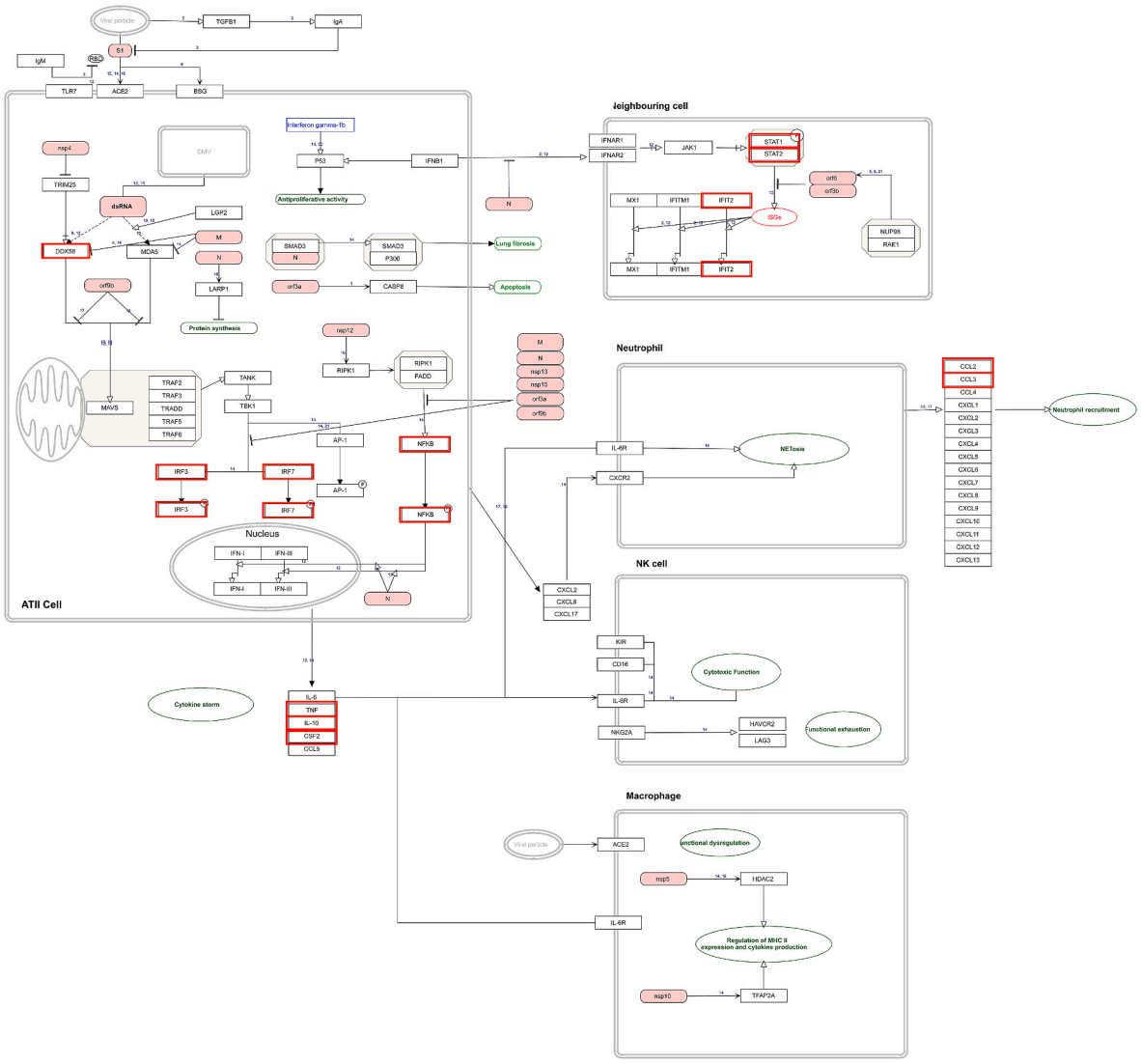

Fig. 5. The biological pathways of the "Host Response Signature Network" were enriched and the most overlapping genes were "SARS-CoV-2 innate immunity evasion and cell-specific immune response pathway".

was a significant difference between the two sample groups regarding dispersion and fold change using DESeq2.

To consider the host gene as a differentially expressed gene, we set the criterion log2 Fold Change |log2FC |> 1.5 and an adjusted p-value <0.05. We selected a meaningful fraction of all DEHGs expression data and converted it into a Z-score (row spacing of values), and then used the pheatmap (version 1.0.12) package in R to create a heat map of this data. We created an MA diagram with the ggplot2 package (version 3.4.0) in R. We created the volcano map of gene expression with the Enhanced-Volcano package (version 1.10.0) in R.

4.2. Functional enrichment analyses

We conducted GO and KEGG pathway analysis using the R package clusterProfiler (version 4.0.5). We set the adjusted P for GO terms and KEGG pathway to less than 0.05 and presented using the R package ggplot2 (version 3.4.0). And analyzed BIOCARTA and DISEASE using the David database (https://david.ncifcrf.gov).

4.3. Analysis of protein-protein interaction (PPI) network and sub-gene cluster screening

We imported differential genes into STRING to acquire a map of the PPI network, and the ppi was set to 0.7 [39]. We imported the results of the STRING analysis of the PPI network into Cytoscape (v.3.9.1), and we clustered the proteins of the PPI network using the Molecular Complexity Detection (MCODE) plugin [40]. We imported the genes in the cluster into STRING, and we mapped the protein interaction network to determine which biological processes obtained by MCODE are involved in the highest-scoring gene clusters. We further analyzed and calculated the resulting gene clusters using the plug-in Network Analyst [41].

4.4. Identification of upstream master regulators of cluster 1 proteins using Cytoscape's plugin

We used the Cytoscape iRegulone plugin (version 1.3) with parameters set to default values to find upstream TF regulators of the Cluster 1 gene [42]. We then summarized and analyzed the iRegulone results, and we visualized the results as a heat map using Morpheus' web tool (https://software.broadinstitute.org/morpheus/). A "host response

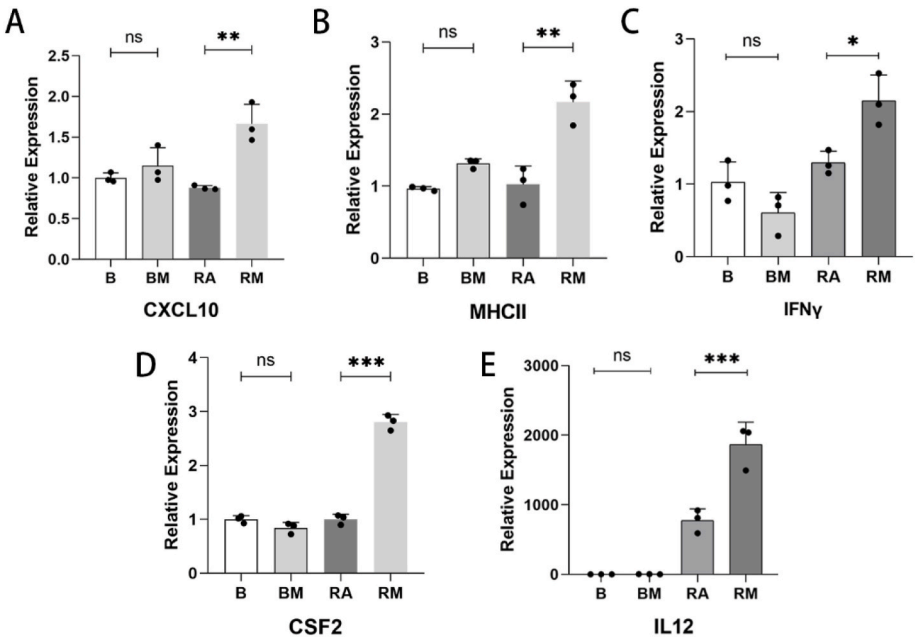

Fig. 6. qRT-PCR experiments were performed on mRNAs from the Ra and RM groups, B and BM represent the Blank group and manganese ion-treated Blank group, respectively. The expression levels of CXCL10, MHCII, IFN-γ, CSF2, and IL12 were measured. In the RM group, the expression levels of all five genes were higher than those in the Ra group: (A) CXCL10, (B) MHCII, (C) IFN-γ, (D) CSF2, and (E) IL12.

signature network" is defined as the 24 proteins contained in group 1 and their upstream TFs.

4.5. Biological pathways for enriching "host response signature networks" using NDEx

The NDEx Project provides an open-source framework where scientists and organizations can store, share, manipulate, and publish biological network knowledge. Genes from the "Host Response Characterization Network" (including upstream regulators) were uploaded to the "relevant pathways" module of the Network Data Exchange for enrichment analysis to identify relevant biological pathways [44, 45]. The output was presented by three main similarity rankings between the query set and network genes, the p-value, and several overlapping genes. The first nine pathways with significant enrichment of five or more overlapping genes were then selected for the next step of the mining analysis. The WikiPathways were also revised using PathVisio (3.3.0).

4.6. Quantitative reverse transcription polymerase chain reaction (qRT-PCR) for validation

To verify the precision of the results obtained from our data analysis, we performed qPCR experiments based on the previous treatments. Human macrophages (THP-1) were divided into the Ra group (single H37Ra infected group) and RM group (manganese ion treated group after being infected by H37Ra), and RNA was extracted using the E. Z.N. A Total RNA Kit I (Omega Bio-Tek, USA). Reverse transcription was performed using Servicebio's Reverse Transcription Kit SweSccipt ALL-in-one First-Strand cDNA Synthesis SuperMix for qPCR, 2xUniversal Blue SYBR Green qPCR Master Mix, and the ABI 7500 Real-time PCR System (Applied Biosystems) for real-time PCR (95 °C, 30 s; 95 °C, 15 s; 60 °C, 30 s, 40 cycles). The relative expression of each selected mRNA between the Ra and RM groups was determined using the 2-ΔΔCt method. β-actin was used as an internal control. The sequences of all primers used in this study are shown below:

Primers.

- β-actin forward 5′-AGCGAGCATCCCCCAAAGTT-3′ and reverse 5′-GGGCACGAAGGCTCATCATT-3′
- IFN-γ forward 5′-TCGGTAACTGACTTGAATGTCCA-3′ and reverse 5′-TCGCTTCCCTGTTTTAGCTGC-3′
- IL-12 forward 5′-TGCCCATTGAGGTCATGGTG-3′ and reverse 5′-CTTGGGTGGGTCAGGTTTGA-3′
- CXCL10 forward 5′-GGTGAGAAGAGATGTCTGAATCC-3′ and reverse 5′-GTCCATCCTTGGAAGCACTGCA-3′
- CSF2 forward 5′-TCCTGAACCTGAGTAGAGACAC-3′ and reverse 5′-TGCTGCTTGTAGTGGCTGG-3′
- MHCII forward 5′-TGTTTGACTTTGATGGTGATGAG-3′ and reverse 5′-AATAATGATGCCCA CCAGACC-3′

5. Conclusions

In this study, we utilized bioinformatics and systems biology to identify differential genes in manganese ion-treated *Mycobacterium tuberculosis*-infected macrophages compared to single-infected cells. Using analytical tools such as STRING and Cytoscape, we obtained the regulatory network Cluster1, which we collectively referred to as the "host response signature network" along with its upstream transcriptional regulators. In a subsequent study, we found that the "host response signature network" was notably correlated with the "immune response to tuberculosis" and "SARS-CoV-2 innate immunity evasion and cell-specific immune response". This indicates that the "host response signature network" obtained from our research was closely related to the immune response of *Mycobacterium tuberculosis*.

Our study demonstrated that manganese ion treatment of *Mycobacterium tuberculosis*-infected macrophages enhances macrophage killing against *Mycobacterium tuberculosis* mainly through the JAK-STAT1-STAT2 pathway mediated by interferon IFN-γ and its receptor IFNGR, as well as the NF-κB-mediated cytokine release pathway. We also verified our results by detecting the increased expression of IFNγ,IL12, CXCL10,CSF2,MHCII genes by qPCR assay. This study provides greater insight into the regulatory mechanisms by which manganese ions enhance macrophage immunity to infection and may contribute to the development of a better approach to the therapeutic intervention against tuberculosis using manganese ions.

Author contributions

Conception and design: M.W., B.T, J.X. Data analysis and interpretation: L.S., Z.W., G.P, L.W., K.Q. Manuscript writing: J.X., L.S., Z.W.

All authors have read and agreed to the published version of the manuscript.

Funding

This work was supported by the Excellent Talents Supporting Plan in Universities of Anhui Province (gxyq2021189), Anhui Provincial Natural Science Foundation (2108085J17, 2108085QH351), Anhui Province Key Laboratory of Immunology in Chronic Diseases Foundation (KLICD-2023-Z2), Bengbu Medical College Graduate Research Innovation Project (Byycxz22001) and National College Student Innovation and Entrepreneurship Training Program (202110367053).

Declaration of competing interest

The authors declare that they have no known competing financial interests or personal relationships that could have appeared to influence the work reported in this paper.

Data availability

No data was used for the research described in the article.

Appendix A. Supplementary data

Supplementary data to this article can be found online at https://doi.org/10.1016/j.bbrep.2023.101602.

References

[1] R. Singh, S.P. Dwivedi, U.S. Gaharwar, R. Meena, P. Rajamani, T. Prasad, Recent updates on drug resistance in Mycobacterium tuberculosis, J. Appl. Microbiol. 128 (2020) 1547–1567, https://doi.org/10.1111/jam.14478.

[2] R. Domingo-Gonzalez, O. Prince, A. Cooper, S.A. Khader, Cytokines and chemokines in Mycobacterium tuberculosis infection, Microbiol. Spectr. 4 (2016), https://doi.org/10.1128/microbiolspec.TBTB2-0018-2016.

[3] M.T. Orr, H.P. Windish, E.A. Beebe, D. Argilla, P.W. Huang, V.A. Reese, S.G. Reed, R.N. Coler, Interferon gamma and tumor necrosis factor are not essential parameters of CD4+ T-cell responses for vaccine control of tuberculosis, J. Infect. Dis. 212 (2015) 495–504, https://doi.org/10.1093/infdis/jiv055.

[4] A.G. Bean, D.R. Roach, H. Briscoe, M.P. France, H. Korner, J.D. Sedgwick, W. J. Britton, Structural deficiencies in granuloma formation in TNF gene-targeted mice underlie the heightened susceptibility to aerosol Mycobacterium tuberculosis infection, which is not compensated for by lymphotoxin, J. Immunol. 162 (1999) 3504–3511.

[5] S.Y. Zhang, S. Boisson-Dupuis, A. Chapgier, K. Yang, J. Bustamante, A. Puel, C. Picard, L. Abel, E. Jouanguy, J.L. Casanova, Inborn errors of interferon (IFN)-mediated immunity in humans: insights into the respective roles of IFN-alpha/beta, IFN-gamma, and IFN-lambda in host defense, Immunol. Rev. 226 (2008) 29–40, https://doi.org/10.1111/j.1600-065X.2008.00698.x.

[6] O. Filipe-Santos, J. Bustamante, A. Chapgier, G. Vogt, L. de Beaucoudrey, J. Feinberg, E. Jouanguy, S. Boisson-Dupuis, C. Fieschi, C. Picard, J.L. Casanova, Inborn errors of IL-12/23- and IFN-gamma-mediated immunity: molecular, cellular, and clinical features, Semin. Immunol. 18 (2006) 347–361, https://doi.org/10.1016/j.smim.2006.07.010.

[7] I. Sologuren, S. Boisson-Dupuis, J. Pestano, Q.B. Vincent, L. Fernandez-Perez, A. Chapgier, M. Cardenes, J. Feinberg, M.I. Garcia-Laorden, C. Picard, E. Santiago, X. Kong, L. Janniere, E. Colino, E. Herrera-Ramos, A. Frances, C. Navarrete, S. Blanche, E. Faria, P. Remiszewski, A. Cordeiro, A. Freeman, S. Holland, K. Abarca, M. Valeron-Lemaur, J. Goncalo-Marques, L. Silveira, J.M. Garcia-Castellano, J. Caminero, J.L. Perez-Arellano, J. Bustamante, L. Abel, J.L. Casanova, C. Rodriguez-Gallego, Partial recessive IFN-gammaR1 deficiency: genetic, immunological and clinical features of 14 patients from 11 kindreds, Hum. Mol. Genet. 20 (2011) 1509–1523, https://doi.org/10.1093/hmg/ddr029.

[8] A.M. Cooper, D.K. Dalton, T.A. Stewart, J.P. Griffin, D.G. Russell, I.M. Orme, Disseminated tuberculosis in interferon gamma gene-disrupted mice, J. Exp. Med. 178 (1993) 2243–2247, https://doi.org/10.1084/jem.178.6.2243.

[9] M. Travar, M. Petkovic, A. Verhaz, Type I, II, and III interferons: regulating immunity to Mycobacterium tuberculosis infection, Arch. Immunol. Ther. Exp. 64 (2016) 19–31, https://doi.org/10.1007/s00005-015-0365-7.

[10] A.E. Abdalla, N. Lambert, X. Duan, J. Xie, Interleukin-10 family and tuberculosis: an old story renewed, Int. J. Biol. Sci. 12 (2016) 710–717, https://doi.org/10.7150/ijbs.13881.

[11] K. Qian, L. Shan, S. Shang, T. Li, S. Wang, M. Wei, B. Tang, J. Xi, Manganese enhances macrophage defense against Mycobacterium tuberculosis via the STING-TNF signaling pathway, Int. Immunopharm. 113 (2022), 109471, https://doi.org/10.1016/j.intimp.2022.109471.

[12] J.Y. Cui, G.P. Lisi, Molecular level insights into the structural and dynamic factors driving cytokine function, Front. Mol. Biosci. 8 (2021), 773252, https://doi.org/10.3389/fmolb.2021.773252.

[13] M. Danilo, V. Chennupati, J.G. Silva, S. Siegert, W. Held, Suppression of tcf1 by inflammatory cytokines facilitates effector CD8 T cell differentiation, Cell Rep. 22 (2018) 2107–2117, https://doi.org/10.1016/j.celrep.2018.01.072.

[14] M.S. Godfrey, L.N. Friedman, Tuberculosis and biologic therapies: anti-tumor necrosis factor-alpha and beyond, Clin. Chest Med. 40 (2019) 721–739, https://doi.org/10.1016/j.ccm.2019.07.003.

[15] H. Luukinen, M.M. Hammaren, L.M. Vanha-Aho, A. Svorjova, L. Kantanen, S. Jarvinen, B.V. Luukinen, E. Dufour, M. Ramet, V.P. Hytonen, M. Parikka, Priming of innate antimycobacterial immunity by heat-killed Listeria monocytogenes induces sterilizing response in the adult zebrafish tuberculosis model, Dis Model Mech 11 (2018), https://doi.org/10.1242/dmm.031658.

[16] H. Clay, H.E. Volkman, L. Ramakrishnan, Tumor necrosis factor signaling mediates resistance to mycobacteria by inhibiting bacterial growth and macrophage death, Immunity 29 (2008) 283–294, https://doi.org/10.1016/j.immuni.2008.06.011.

[17] A.C. Rothchild, B. Stowell, G. Goyal, C. Nunes-Alves, Q. Yang, K. Papavinasasundaram, C.M. Sassetti, G. Dranoff, X. Chen, J. Lee, S.M. Behar, Role of granulocyte-macrophage colony-stimulating factor production by T cells during Mycobacterium tuberculosis infection, mBio 8 (2017), https://doi.org/10.1128/mBio.01514-17.

[18] V. Dwivedi, S. Gautam, C.A. Headley, T. Piergallini, J.B. Torrelles, J. Turner, IL-10 receptor blockade delivered simultaneously with Bacillus calmette-guerin vaccination sustains long-term protection against Mycobacterium tuberculosis infection in mice, J. Immunol. 208 (2022) 1406–1416, https://doi.org/10.4049/jimmunol.2100900.

[19] K. Harling, E. Adankwah, A. Guler, A. Afum-Adjei Awuah, L. Adu-Amoah, E. Mayatepek, E. Owusu-Dabo, N. Nausch, M. Jacobsen, Constitutive STAT3 phosphorylation and IL-6/IL-10 co-expression are associated with impaired T-cell function in tuberculosis patients, Cell. Mol. Immunol. 16 (2019) 275–287, https://doi.org/10.1038/cmi.2018.5.

[20] Y. Liu, Z. Liu, H. Tang, Y. Shen, Z. Gong, N. Xie, X. Zhang, W. Wang, W. Kong, Y. Zhou, Y. Fu, The N(6)-methyladenosine (m(6)A)-forming enzyme METTL3 facilitates M1 macrophage polarization through the methylation of STAT1 mRNA, Am J Physiol Cell Physiol 317 (2019) C762–C775, https://doi.org/10.1152/ajpcell.00212.2019.

[21] X.H. Yi, B. Zhang, Y.R. Fu, Z.J. Yi, STAT1 and its related molecules as potential biomarkers in Mycobacterium tuberculosis infection, J. Cell Mol. Med. 24 (2020) 2866–2878, https://doi.org/10.1111/jcmm.14856.

[22] A.I. Rovetta, D. Pena, R.E. Hernandez Del Pino, G.M. Recalde, J. Pellegrini, F. Bigi, R.M. Musella, D.J. Palmero, M. Gutierrez, M.I. Colombo, V.E. Garcia, IFNG-mediated immune responses enhance autophagy against Mycobacterium tuberculosis antigens in patients with active tuberculosis, Autophagy 10 (2014) 2109–2121, https://doi.org/10.4161/15548627.2014.981791.

[23] N. Ahamad, P.C. Rath, Expression of interferon regulatory factors (IRF-1 and IRF-2) during radiation-induced damage and regeneration of bone marrow by transplantation in mouse, Mol. Biol. Rep. 46 (2019) 551–567, https://doi.org/10.1007/s11033-018-4508-x.

[24] H.S. Chiang, H.M. Liu, The molecular basis of viral inhibition of IRF- and STAT-dependent immune responses, Front. Immunol. 9 (2018) 3086, https://doi.org/10.3389/fimmu.2018.03086.

[25] J. Rosain, A.L. Neehus, J. Manry, R. Yang, J. Le Pen, W. Daher, Z. Liu, Y.H. Chan, N. Tahuil, O. Turel, M. Bourgey, M. Ogishi, J.M. Doisne, H.M. Izquierdo, T. Shirasaki, T. Le Voyer, A. Guerin, P. Bastard, M. Moncada-Velez, J.E. Han, T. Khan, F. Rapaport, S.H. Hong, A. Cheung, K. Haake, B.C. Mindt, L. Perez, Q. Philippot, D. Lee, P. Zhang, D. Rinchai, F. Al Ali, M.M. Ahmad Ata, M. Rahman, J.N. Peel, S. Heissel, H. Molina, Y. Kendir-Demirkol, R. Bailey, S. Zhao, J. Bohlen, M. Mancini, Y. Seeleuthner, M. Roelens, L. Lorenzo, C. Soudee, M.E.J. Paz, M. L. Gonzalez, M. Jeljeli, J. Soulier, S. Romana, A.S. L'Honneur, M. Materna, R. Martinez-Barricarte, M. Pochon, C. Oleaga-Quintas, A. Michev, M. Migaud, R. Levy, M.A. Alyanakian, F. Rozenberg, C.A. Croft, G. Vogt, J.F. Emile, L. Kremer, C.S. Ma, J.H. Fritz, S.M. Lemon, A.N. Spaan, N. Manel, L. Abel, M.R. MacDonald, S. Boisson-Dupuis, N. Marr, S.G. Tangye, J.P. Di Santo, Q. Zhang, S.Y. Zhang, C. M. Rice, V. Beziat, N. Lachmann, D. Langlais, J.L. Casanova, P. Gros, J. Bustamante, Human IRF1 governs macrophagic IFN-gamma immunity to mycobacteria, Cell 186 (2023) 621–645 e633, https://doi.org/10.1016/j.cell.2022.12.038.

[26] D.A. Banks, S.E. Ahlbrand, V.K. Hughitt, S. Shah, K.D. Mayer-Barber, S.N. Vogel, N. M. El-Sayed, V. Briken, Mycobacterium tuberculosis inhibits autocrine type I IFN signaling to increase intracellular survival, J. Immunol. 202 (2019) 2348–2359, https://doi.org/10.4049/jimmunol.1801303.

[27] S. BoseDasgupta, J. Pieters, Macrophage-microbe interaction: lessons learned from the pathogen Mycobacterium tuberculosis, Semin. Immunopathol. 40 (2018) 577–591, https://doi.org/10.1007/s00281-018-0710-0.

[28] A. Giraud-Gatineau, J.M. Coya, A. Maure, A. Biton, M. Thomson, E.M. Bernard, J. Marrec, M.G. Gutierrez, G. Larrouy-Maumus, R. Brosch, B. Gicquel, L. Tailleux, The antibiotic bedaquiline activates host macrophage innate immune resistance to bacterial infection, Elife 9 (2020), https://doi.org/10.7554/eLife.55692.

[29] C. Genestet, F. Bernard-Barret, E. Hodille, C. Ginevra, F. Ader, S. Goutelle, G. Lina, O. Dumitrescu, T.B.s.g. Lyon, Antituberculous drugs modulate bacterial phagolysosome avoidance and autophagy in Mycobacterium tuberculosis-infected macrophages, Tuberculosis 111 (2018) 67–70, https://doi.org/10.1016/j.tube.2018.05.014.

[30] Y. Cheng, J.S. Schorey, Mycobacterium tuberculosis-induced IFN-beta production requires cytosolic DNA and RNA sensing pathways, J. Exp. Med. 215 (2018) 2919–2935, https://doi.org/10.1084/jem.20180508.

[31] W. Si, H. Liang, J. Bugno, Q. Xu, X. Ding, K. Yang, Y. Fu, R.R. Weichselbaum, X. Zhao, L. Wang, Lactobacillus rhamnosus GG induces cGAS/STING- dependent type I interferon and improves response to immune checkpoint blockade, Gut 71 (2022) 521–533, https://doi.org/10.1136/gutjnl-2020-323426.

[32] L. Barnabei, E. Laplantine, W. Mbongo, F. Rieux-Laucat, R. Weil, NF-kappaB: at the borders of autoimmunity and inflammation, Front. Immunol. 12 (2021), 716469, https://doi.org/10.3389/fimmu.2021.716469.

[33] B. Miraghazadeh, M.C. Cook, Nuclear factor-kappaB in autoimmunity: man and mouse, Front. Immunol. 9 (2018) 613, https://doi.org/10.3389/fimmu.2018.00613.

[34] L. Zhang, X. Xiao, P.R. Arnold, X.C. Li, Transcriptional and epigenetic regulation of immune tolerance: roles of the NF-kappaB family members, Cell. Mol. Immunol. 16 (2019) 315–323, https://doi.org/10.1038/s41423-019-0202-8.

[35] K.L. Henry, D. Kellner, B. Bajrami, J.E. Anderson, M. Beyna, G. Bhisetti, T. Cameron, A.G. Capacci, A. Bertolotti-Ciarlet, J. Feng, B. Gao, B. Hopkins, T. Jenkins, K. Li, T. May-Dracka, P. Murugan, R. Wei, W. Zeng, N. Allaire, A. Buckler, C. Loh, P. Juhasz, B. Lucas, K.A. Ennis, E. Vollman, E. Cahir-McFarland, E.C. Hett, M.L. Ols, CDK12-mediated transcriptional regulation of noncanonical NF-kappaB components is essential for signaling, Sci. Signal. 11 (2018), https://doi.org/10.1126/scisignal.aam8216.

[36] H. Yu, L. Lin, Z. Zhang, H. Zhang, H. Hu, Targeting NF-kappaB pathway for the therapy of diseases: mechanism and clinical study, Signal Transduct. Targeted Ther. 5 (2020) 209, https://doi.org/10.1038/s41392-020-00312-6.

[37] X. Zhou, L. Zhang, L. Lie, Z. Zhang, B. Zhu, J. Yang, Y. Gao, P. Li, Y. Huang, H. Xu, Y. Li, X. Du, C. Zhou, S. Hu, Q. Wen, X.P. Zhong, L. Ma, MxA suppresses TAK1-IKKalpha/beta-NF-kappaB mediated inflammatory cytokine production to facilitate Mycobacterium tuberculosis infection, J. Infect. 81 (2020) 231–241, https://doi.org/10.1016/j.jinf.2020.05.030.

[38] M.I. Love, W. Huber, S. Anders, Moderated estimation of fold change and dispersion for RNA-seq data with DESeq2, Genome Biol. 15 (2014) 550, https://doi.org/10.1186/s13059-014-0550-8.

[39] G.D. Bader, C.W. Hogue, An automated method for finding molecular complexes in large protein interaction networks, BMC Bioinf. 4 (2003) 2, https://doi.org/10.1186/1471-2105-4-2.

[40] J. Xia, E.E. Gill, R.E. Hancock, NetworkAnalyst for statistical, visual and network-based meta-analysis of gene expression data, Nat. Protoc. 10 (2015) 823–844, https://doi.org/10.1038/nprot.2015.052.

[41] R. Janky, A. Verfaillie, H. Imrichova, B. Van de Sande, L. Standaert, V. Christiaens, G. Hulselmans, K. Herten, M. Naval Sanchez, D. Potier, D. Svetlichnyy, Z. Kalender Atak, M. Fiers, J.C. Marine, S. Aerts, iRegulon: from a gene list to a gene regulatory network using large motif and track collections, PLoS Comput. Biol. 10 (2014), e1003731, https://doi.org/10.1371/journal.pcbi.1003731.

[42] D. Pratt, J. Chen, D. Welker, R. Rivas, R. Pillich, V. Rynkov, K. Ono, C. Miello, L. Hicks, S. Szalma, A. Stojmirovic, R. Dobrin, M. Braxenthaler, J. Kuentzer, B. Demchak, T. Ideker, NDEx, the network data Exchange, Cell Syst 1 (2015) 302–305, https://doi.org/10.1016/j.cels.2015.10.001.